

Contents

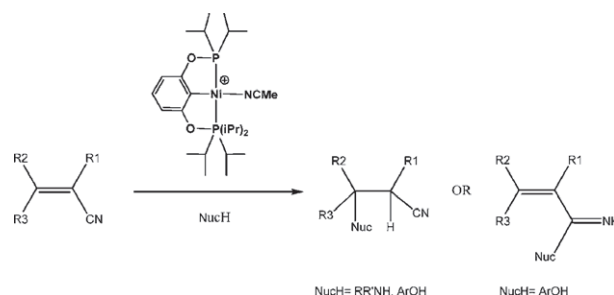
Articles

Xavier Lefèvre, Guillaume Durieux, Stéphanie Lesturgez, Davit Zargarian

Journal of Molecular Catalysis A: Chemical 335 (2011) 1

Addition of amines and phenols to acrylonitrile derivatives catalyzed by the POCOP-type pincer complex $[\{\kappa^P, \kappa^C, \kappa^P\text{-}2,6\text{-}(i\text{-Pr})_2\text{PO}_2\text{C}_6\text{H}_3\}\text{Ni}(\text{NCMe})][\text{OSO}_2\text{CF}_3]$

► Greater range of amine substrates for hydroamination of acrylonitrile and its derivatives. ► First pincer-type nickel complex to promote hydroaryloxylation of acrylonitrile. ► Noted important role played by bases in promoting the hydroaryloxylation reaction. ► Obtained supporting evidence for the proposed mechanism of catalysis. ► Discovered the conversion of nitriles to amidines during the hydroamination catalysis.

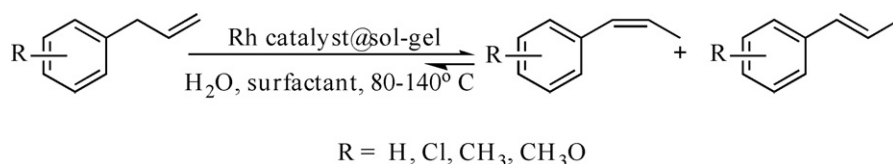


Diana Meltzer, David Avnir, Monzer Fanun, Vitaly Gutkin, Inna Popov, Reinhard Schomäcker, Michael Schwarze, Jochanan Blum

Journal of Molecular Catalysis A: Chemical 335 (2011) 8

Catalytic isomerization of hydrophobic allylarenes in aqueous microemulsions

► Replacement of organic solvents by aqueous microemulsions. ► Catalysis of water insoluble substrates in aqueous media. ► Double bond isomerization in allylarenes.

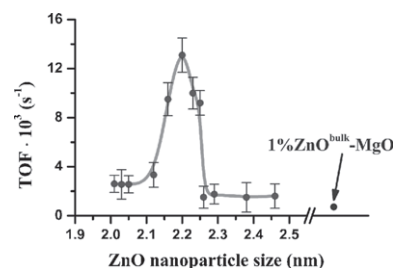


Olga Z. Didenko, Gulnara R. Kosmambetova, Peter E. Strizhak

Journal of Molecular Catalysis A: Chemical 335 (2011) 14

Size effect in CO oxidation over magnesia-supported ZnO nanoparticles

► The bell-shaped size dependence of the catalytic activity of magnesia-supported ZnO nanoparticles (2.0–2.3 nm) in CO oxidation was found and explained by the quantum confinement effect.

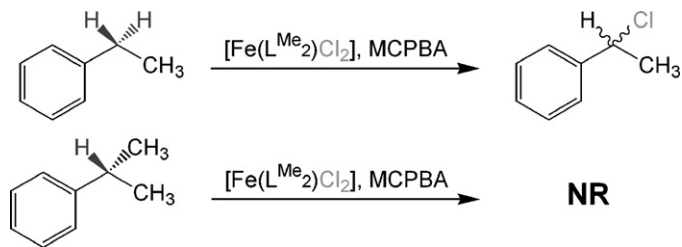


**Christian R. Goldsmith, Cristina M. Coates,
Kenton Hagan, Casey A. Mitchell**

Journal of Molecular Catalysis A: Chemical 335 (2011) 24

Hydrocarbon chlorination promoted by manganese and iron complexes with methylated derivatives of bis(2-pyridylmethyl)-1,2-ethanediamine

- Metal complexes with bispiden derivatives chlorinate benzylic substrates. ► $[M^V(L)(O)Cl_2]$ species are believed to be responsible for the chlorination. ► Iron leads to superior chlorination activity than manganese.
- Increased ligand methylation leads to regioselectivity.

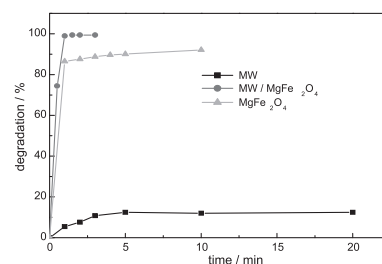


**Lei Zhang, Xinyu Zhou, Xingjia Guo,
Xiaoyan Song, Xueyan Liu**

Journal of Molecular Catalysis A: Chemical 335 (2011) 31

Investigation on the degradation of acid fuchsin induced oxidation by $MgFe_2O_4$ under microwave irradiation

- $MgFe_2O_4$ has high catalytic activity and adsorption capacity. ► $MgFe_2O_4$ acts as a catalyst in the microwave degradation dyes process. ► The degradation of acid fuchsin was an integrated MW/ $MgFe_2O_4$ process.
- Acid fuchsin was rapidly degraded into harmless products in MW/ $MgFe_2O_4$ system.

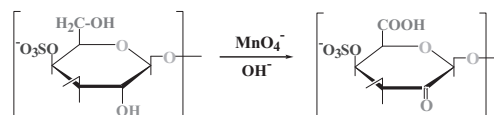


**R.M. Hassan, A. Fawzy, A. Alarifi, G.A. Ahmed,
I.A. Zaafarany, H.D. Takagi**

Journal of Molecular Catalysis A: Chemical 335 (2011) 38

Base-catalyzed oxidation of some sulfated macromolecules: Kinetics and mechanism of formation of intermediate complexes of short-lived manganate (VI) and/or hypomanganate (V) during oxidation of iota- and lambda-carrageenan polysaccharides by alkaline permanganate

- The kinetics and mechanistic of oxidation of some sulfated macromolecules by alkaline permanganate.
- Novel synthesis of keto-acid derivatives of iota- and lambda-carrageenans by oxidation processes.
- Spectrophotometric detection of short-lived Mn^V and Mn^{VI} intermediates using a conventional spectrophotometer. ► Behavior of sulfated polysaccharides in aqueous alkaline solutions.

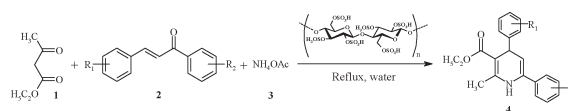


**Javad Safari, Sayed Hossein Banitaba,
Shiva D. Khalili**

Journal of Molecular Catalysis A: Chemical 335 (2011) 46

Cellulose sulfuric acid catalyzed multicomponent reaction for efficient synthesis of 1,4-dihydropyridines via unsymmetrical Hantzsch reaction in aqueous media

- The natural biopolymers was used as solid support catalyst. ► Cellulose sulfuric acid catalyzed synthesis of 1,4-dihydropyridines. ► Suspension of catalyst in water was effective on yield of reaction. ► Catalyst can be easily separated and reused several times in subsequent reactions.

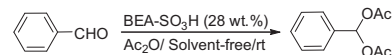


Roozbeh Javad Kalbasi, Ahmad Reza Massah, Anahita Shafiei

Journal of Molecular Catalysis A: Chemical 335 (2011) 51

Synthesis and characterization of BEA-SO₃H as an efficient and chemoselective acid catalyst

► BEA-SO₃H was prepared with various amounts of chlorosulphonic acid without using organosilica and bridged organosilane precursors. ► BEA-SO₃H catalyst showed good yield at very short time for the synthesis and deprotection of 1,1-diacetates. ► BEA-SO₃H was found to be recyclable for the protection of aldehydes with acetic anhydride. ► BEA-SO₃H showed good chemo-selectivity and shape-selectivity for the preparation of 1,1-diacetates.

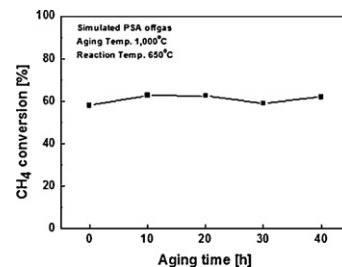


Seongmin Kim, Dae-Won Lee, Joon Yeob Lee, Hee-Jun Eom, Hwa Jung Lee, In-ho Cho, Kwan-Young Lee

Journal of Molecular Catalysis A: Chemical 335 (2011) 60

Catalytic combustion of methane in simulated PSA offgas over Mn-substituted La-Sr-hexaaluminate (La_xSr_{1-x}MnAl₁₁O₁₉)

► The combustion activity of hexaaluminate was dependent on its surface area. ► Throughout a thermal aging test, the activity of La_{0.6}Sr_{0.4}MnAl₁₁O₁₉ remained constant. ► La_{0.6}Sr_{0.4}MnAl₁₁O₁₉ was stable after the thermal aging test under simulated PSA offgas.

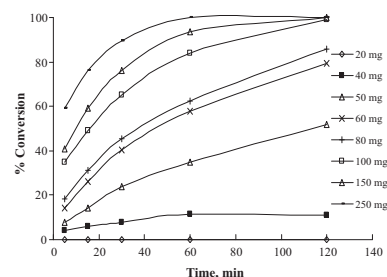


Sumeet K. Sharma, Kalpesh B. Sidhpuria, Raksh V. Jasra

Journal of Molecular Catalysis A: Chemical 335 (2011) 65

Ruthenium containing hydrotalcite as a heterogeneous catalyst for hydrogenation of benzene to cyclohexane

► Ru-HT synthesized by partial substitution of Mg²⁺ or Al³⁺ cations by ruthenium metal in octahedral layers of hydrotalcite. ► Ru-HT as a reusable heterogeneous catalyst for hydrogenation of benzene. ► Complete conversion of benzene with 100% selectivity to cyclohexane. ► Kinetic study for liquid phase hydrogenation of benzene.

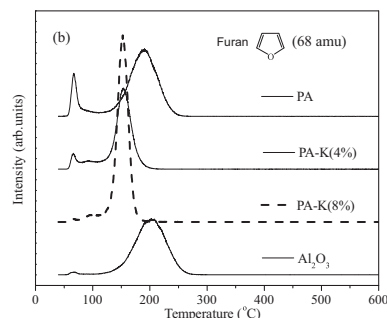


Wei Zhang, Yulei Zhu, Shasha Niu, Yongwang Li

Journal of Molecular Catalysis A: Chemical 335 (2011) 71

A study of furfural decarbonylation on K-doped Pd/Al₂O₃ catalysts

► The yield of furan is 99.5% at 260 °C on Pd-K₂CO₃/Al₂O₃ (K% = 8 wt.%) catalyst. ► The selectivity of 2-methylfuran will be zero at higher K-content catalysts. ► Furfural-TPSR indicates that K-doped catalysts promote furfural decarbonylation. ► Furfural-FTIR shows that K-doped catalysts change the adsorption mode of furfural. ► The decrease of η₂(C,O)-furfural by K-doping inhibits furfural hydrogenation.

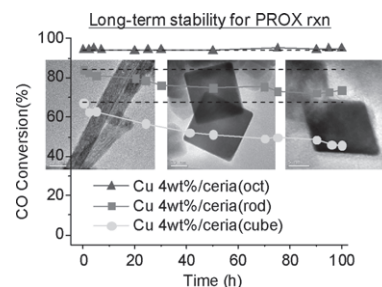


Jaeman Han, Hyung Jun Kim, Sangwoon Yoon, Hyunjoon Lee

Journal of Molecular Catalysis A: Chemical 335 (2011) 82

Shape effect of ceria in Cu/ceria catalysts for preferential CO oxidation

► Different shapes of ceria supports (rods, cubes, and octahedra) were synthesized. ► The deposition mode of copper was different depending on the ceria shape. ► Activity and long-term stability were tested for PROX reaction by using Cu/ceria. ► Cu/ceria-octahedra showed the best activity and long-term stability.

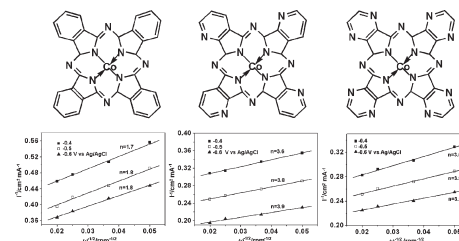


Zhanwei Xu, Hejun Li, Gaoxiang Cao, Qinglin Zhang, Kezhi Li, Xueni Zhao

Journal of Molecular Catalysis A: Chemical 335 (2011) 89

Electrochemical performance of carbon nanotube-supported cobalt phthalocyanine and its nitrogen-rich derivatives for oxygen reduction

► MWCNT-supported CoPc derivatives are prepared by solid phase synthesis method. ► MWCNT-supported CoPc shows a two-step, two-electron process for ORR. ► MWCNT-supported CoTAP and CoPTpz exhibit a one-step, four-electron pathway for ORR. ► MWCNT-supported CoTAP and CoPTpz have higher activity to ORR among them.

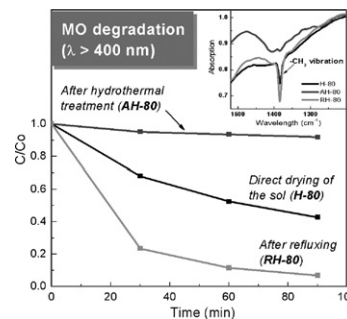


Jingjing Jiang, Mingce Long, Deyong Wu, Weimin Cai

Journal of Molecular Catalysis A: Chemical 335 (2011) 97

Alkoxy-derived visible light activity of TiO₂ synthesized at low temperature

► Visible-light-activated TiO₂ synthesized without external doping source. ► Alkoxy-derived surface states formed in a low-temperature synthetic process. ► Visible-light induced charge transfer contributed to the photocatalytic reactions.

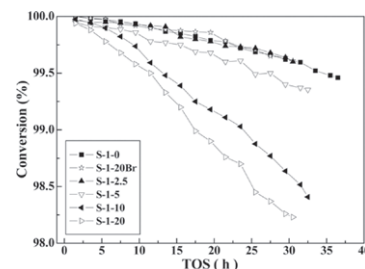


Fanhui Meng, Yaquan Wang, Lina Wang, Rumin Yang, Teng Zhang

Journal of Molecular Catalysis A: Chemical 335 (2011) 105

Influence of Br⁻ and Na⁺ in synthesis of Silicalite-1 on catalytic performance in vapor phase Beckmann rearrangement of cyclohexanone oxime

► Presence of Br⁻ in synthesis does not influence properties and performance of S-1. ► Presence of high concentration Na⁺ in synthesis increases the particle sizes of S-1. ► S-1 synthesized in the presence of high concentrations of Na⁺ deactivate faster. ► Na⁺ below 2.5 mol% of TPAOH can be tolerated in synthesis of S-1 as catalyst.

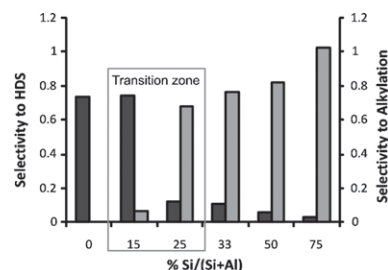


David J. Pérez-Martínez, Eric M. Gaigneaux, Sonia A. Giraldo, Aristóbulo Centeno

Journal of Molecular Catalysis A: Chemical 335 (2011) 112

Interpretation of the catalytic functionalities of CoMo/ASA FCC-naphtha-HDT catalysts based on its acid properties

► CoMo/ASA catalysts were evaluated in the HDT of synthetic FCC naphtha. ► A kind of transition zone between HDS-type and acid-type catalysts was found. ► This transition zone was located between 15 and 25% Si/(Si + Al). ► The transition zone was related with an increment in the Brønsted acidity.

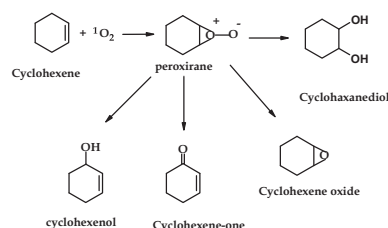


Vongani P. Chauke, Edith Antunes, Wadzana Chidawanyika, Tebello Nyokong

Journal of Molecular Catalysis A: Chemical 335 (2011) 121

Photocatalytic behaviour of tantalum (V) phthalocyanines in the presence of gold nanoparticles towards the oxidation of cyclohexene

► Au nanoparticles improve singlet oxygen quantum yields of Ta phthalocyanine. ► Ta phthalocyanine – Au nanoparticles catalyse the photooxidation of cyclohexene. ► Cyclohexene oxide, cyclohexenol, cyclohexanone and cyclohexanediol are formed. ► Ta phthalocyanine show stability during the photocatalysis.

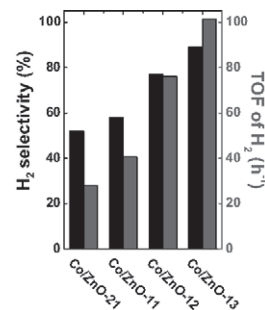


Xianwen Chu, Jun Liu, Bo Sun, Rui Dai, Yan Pei, Minghua Qiao, Kangnian Fan

Journal of Molecular Catalysis A: Chemical 335 (2011) 129

Aqueous-phase reforming of ethylene glycol on Co/ZnO catalysts prepared by the coprecipitation method

► Co/ZnO catalysts were prepared by the coprecipitation method. ► They exhibit high intrinsic activity and H₂ selectivity in APR of ethylene glycol. ► The reaction pathways are discussed.

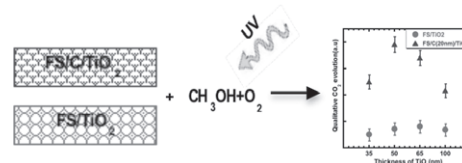


Raja Sellappan, Jiefang Zhu, Hans Fredriksson, Rafael S. Martins, Michael Zäch, Dinko Chakarov

Journal of Molecular Catalysis A: Chemical 335 (2011) 136

Preparation and characterization of TiO₂/carbon composite thin films with enhanced photocatalytic activity

► Photocatalytic oxidation of methanol on composite (C + TiO₂) and pure TiO₂ film. ► Composite films show an enhanced photoactivity than pure TiO₂. ► Enhancement is due to synergy effect of carbon at the TiO₂ nanocrystals interface. ► The effect restricts crystal growth of TiO₂ and contributes to charge separation.

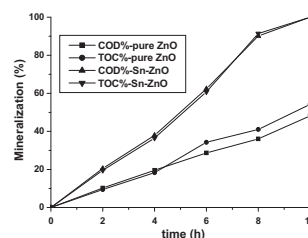


Jian-Hui Sun, Shu-Ying Dong, Jing-Lan Feng, Xiao-Jing Yin, Xiao-Chuan Zhao

Journal of Molecular Catalysis A: Chemical 335 (2011) 145

Enhanced sunlight photocatalytic performance of Sn-doped ZnO for Methylene Blue degradation

► Nano-structured ZnO and Sn-doped ZnO photocatalysts were successfully synthesized by microwave heating. ► The doping greatly changed the microstructure, morphology and optical properties of ZnO. ► The photocatalytic activity of the prepared pure ZnO and Sn-doped ZnO were investigated by the degradation of Methylene Blue (MB) under sunlight irradiation. ► Compared with pure ZnO, 13% higher decolorization rate and 29–52% higher mineralization efficiency were obtained by the Sn-doped ZnO. ► Sn-doped ZnO had a higher photocatalytic activity and Sn dopant greatly increased the photocatalytic activity of ZnO.

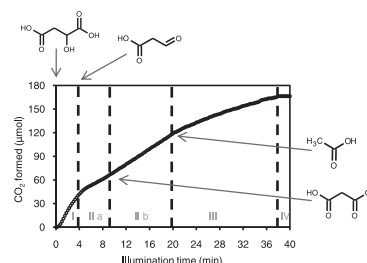


Wenny Irawaty, Donia Friedmann, Jason Scott, Rose Amal

Journal of Molecular Catalysis A: Chemical 335 (2011) 151

Relationship between mineralization kinetics and mechanistic pathway during malic acid photodegradation

► Malic acid mineralization profile possesses varying mineralization rates. ► The mineralization rates depend on the dominant intermediate present in the solution. ► The affinity of the intermediates to TiO₂ surface together with their structure affect the mineralization kinetics.

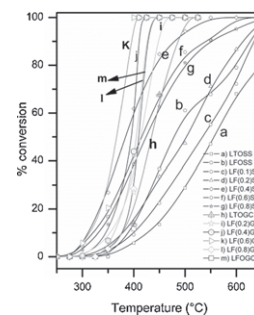


K.K. Kartha, M.R. Pai, A.M. Banerjee, R.V. Pai, S.S. Meena, S.R. Bharadwaj

Journal of Molecular Catalysis A: Chemical 335 (2011) 158

Modified surface and bulk properties of Fe-substituted lanthanum titanates enhances catalytic activity for CO + N₂O reaction

► Nominal compositions La₂Ti_{1-x}Fe_{2x}O_{7-δ} by gel combustion, solid state route. ► Transition from La₂Ti₂O₇ to LaFeO₃ single phase beyond 40–60% Fe content. ► Maximum activity over LF(0.6)GC for decomposition of N₂O using CO. ► Substitution-induced anionic vacancies, asymmetric environment around Fe. ► Surface–bulk-activity correlations.

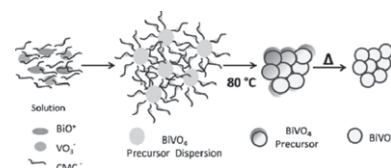


U.M. García Pérez, S. Sepúlveda-Guzmán, A. Martínez-de la Cruz, U. Ortiz Méndez

Journal of Molecular Catalysis A: Chemical 335 (2011) 169

Photocatalytic activity of BiVO₄ nanospheres obtained by solution combustion synthesis using sodium carboxymethylcellulose

► This work is in the direction of searching alternative materials to take advantage of the solar energy. ► We propose the use of sodium carboxymethylcellulose as additive during the BiVO₄ synthesis. ► The prepared BiVO₄ nanospheres exhibited high photocatalytic activity under visible irradiation. ► The analysis of TOC showed that the mineralization of rhB over a BiVO₄ photocatalyst is feasible.

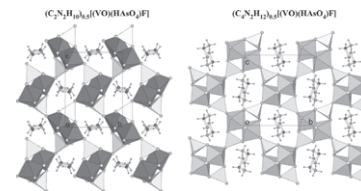


Teresa Berrocal, Edurne S. Larrea, Marta Iglesias, Maria I. Arriortua

Journal of Molecular Catalysis A: Chemical 335 (2011) 176

Vanadyl arsenates as catalysts for selective oxidation of organic sulfides and alkenes

► EnVAs and PipVAs were tested as heterogeneous catalysts with good results. ► EnVAs is more efficient than PipVAs. ► This difference is consequence of the structural differences between both catalysts. ► Both catalysts can be reused without losing their activity.

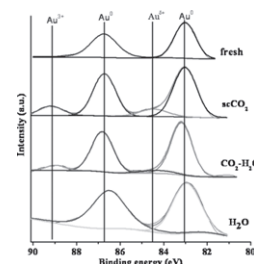


Yufen Hao, Ruixia Liu, Xiangchun Meng, Haiyang Cheng, Fengyu Zhao

Journal of Molecular Catalysis A: Chemical 335 (2011) 183

Deactivation of Au/TiO₂ catalyst in the hydrogenation of *o*-chloronitrobenzene in the presence of CO₂

► The catalytic performance of Au/TiO₂ catalyst was discussed in the presence of supercritical carbon dioxide. ► Au/TiO₂ is confirmed to deactivate during the hydrogenation of *o*-chloronitrobenzene in scCO₂. ► Several factors were proposed to arouse the decrease of activity of Au/TiO₂ catalyst: (a) carbonate-like species are formed on gold; (b) the Au⁰ species is partially oxidized by CO₂ even in the presence of H₂, (c) CO might be formed in the hydrogenation process and poisons some active sites.

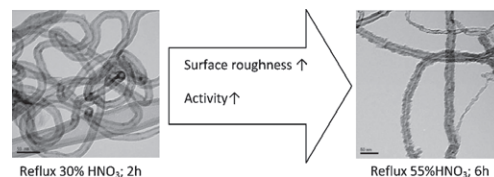


Myriam A.M. Motchelaho, Haifeng Xiong, Mahluli Moyo, Linda L. Jewell, Neil J. Coville

Journal of Molecular Catalysis A: Chemical 335 (2011) 189

Effect of acid treatment on the surface of multiwalled carbon nanotubes prepared from Fe–Co supported on CaCO₃: Correlation with Fischer–Tropsch catalyst activity

► Carbon nanotubes were acid refluxed with two different HNO₃ concentrations and times. As the severity of acid treatment of carbon nanotubes increases: ► the surface morphology becomes rougher and the material becomes less crystalline. ► The amount of surface oxygen groups increases and the thermal stability decreases. ► The activity of 10% Fe/CNT for Fischer–Tropsch synthesis increases significantly. ► The methane selectivity decreases and the C₅₊ selectivity increases.

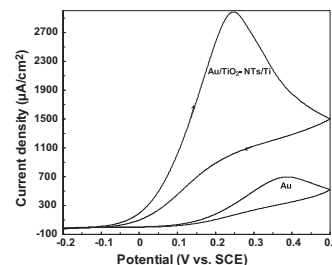


Mirghasem Hosseini, Mohamad Mohsen Momeni, Masoud Faraji

Journal of Molecular Catalysis A: Chemical 335 (2011) 199

Electro-oxidation of hydrazine on gold nanoparticles supported on TiO₂ nanotube matrix as a new high active electrode

► Au/TiO₂-NTs/Ti catalysts with highly porous structure and excellent electro-catalytic property have been successfully fabricated by a two-step process consisting of anodizing titanium followed by electroplating of gold. ► Due to the uniform dispersion of gold nanoparticles on TiO₂-NTs, smaller particle size and unique properties of TiO₂-NTs support, Au/TiO₂-NTs/Ti electrode have High current density and good stability toward electro-oxidation of hydrazine. ► The oxidation kinetic of hydrazine on Au/TiO₂-NTs/Ti electrode was studied and results indicated that the oxidation process is diffusion controlled. ► This study provides a promising route for the simple, facile and cost-effective synthesis of Au/TiO₂-NTs/Ti catalysts and the as-synthesized catalysts show great prospect in the applications of fuel cells.

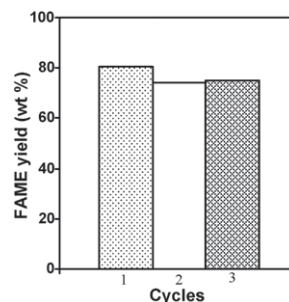


Antonio Jiménez-López, Ignacio Jiménez-Morales, José Santamaría-González, Pedro Maireles-Torres

Journal of Molecular Catalysis A: Chemical 335 (2011) 205

Biodiesel production from sunflower oil by tungsten oxide supported on zirconium doped MCM-41 silica

► Zirconium doped MCM-41 silica supported WO_x solids are a new family of active acid catalysts for the methanolysis of sunflower oil. ► Their activity is maintained after three catalytic cycles. ► These acid catalysts simultaneously catalyze the esterification of fatty acids and the transesterification of triglycerides.

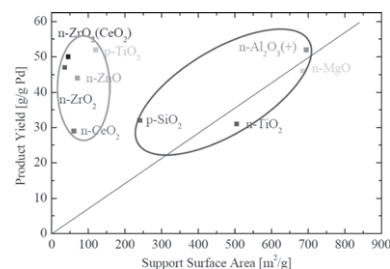


Luke M. Neal, Michael L. Everett, Gar B. Hoflund, Helena E. Hagelin-Weaver

Journal of Molecular Catalysis A: Chemical 335 (2011) 210

Characterization of palladium oxide catalysts supported on nanoparticle metal oxides for the oxidative coupling of 4-methylpyridine

► The XPS data confirm the classification of $n\text{-Al}_2\text{O}_3(+)$, $n\text{-MgO}$ and $p\text{-SiO}_2$ as non-interacting supports and $p\text{-TiO}_2$, $n\text{-ZnO}$, $n\text{-ZrO}_2$, $n\text{-ZrO}_2(\text{CeO}_2)$, and $n\text{-CeO}_2$ as interacting supports. ► For TiO_2 -supported catalysts, the crystal structure of the support appears to be important, with anatase being the desired phase. ► Too strong palladium-support interactions, such as in the case of $\text{PdO}/n\text{-CeO}_2$, can cause migration of support species over the active palladium sites.

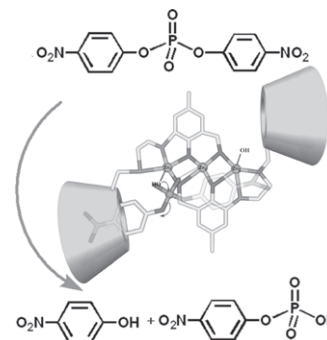


Si-Ping Tang, Ping Hu, Huo-Yan Chen, Sha Chen, Zong-Wan Mao, Liang-Nian Ji

Journal of Molecular Catalysis A: Chemical 335 (2011) 222

Carboxy and diphosphate ester hydrolysis promoted by di- or tri-nuclear zinc(II) complexes based on β -cyclodextrin

► Trinuclear zinc complex based β -cyclodextrins catalyzed ester hydrolysis. The complex displayed good hydrolytic activities for monoester and diesters. The cooperation of metal centers and β -cyclodextrin was important for ester cleavage.

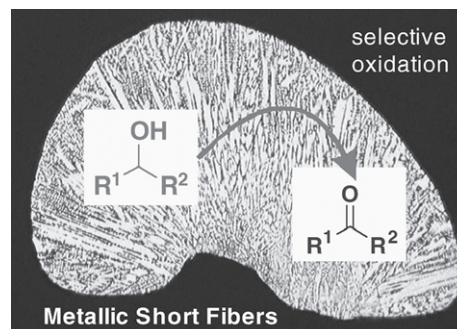


Achim Stolle, Bernd Ondruschka, Ingrid Morgenthal, Olaf Andersen, Werner Bonrath

Journal of Molecular Catalysis A: Chemical 335 (2011) 228

Metallic short fibers for liquid-phase oxidation reactions

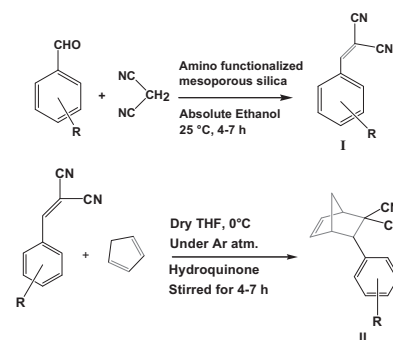
► The production of metallic short fibers (MSF) is a straightforward process. ► MSF are potent catalysts for chemoselective liquid-phase alcohol oxidation. ► Oxidation is possible with the environmentally friendly oxidant hydrogen peroxide. ► Cu_3Sn intermetallic phase was identified as the material with the most promising properties. ► The scope of reactions is extended to liquid-phase epoxidation of olefinic double bonds.



John Mondal, Arindam Modak, Asim Bhaumik*Journal of Molecular Catalysis A: Chemical* 335 (2011) 236

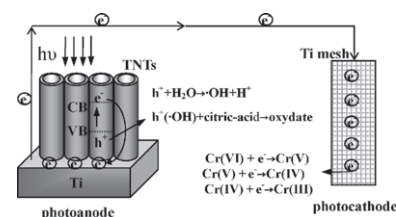
Highly efficient mesoporous base catalyzed Knoevenagel condensation of different aromatic aldehydes with malononitrile and subsequent noncatalytic Diels–Alder reactions

► Synthesis of aminopropyl functionalized mesoporous material. ► Knoevenagel condensation of aromatic aldehydes with malononitrile. ► High yields for α,β -unsaturated dicyanides in this Knoevenagel condensation. ► Efficient Diels–Alder reaction of α,β -unsaturated dicyanides with cyclopentadiene.

**Qing Wang, Jing Shang, Tong Zhu, Fengwei Zhao***Journal of Molecular Catalysis A: Chemical* 335 (2011) 242

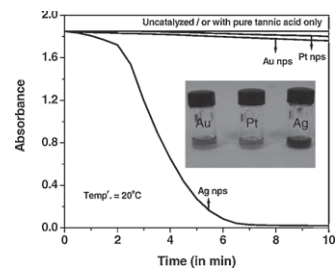
Efficient photoelectrocatalytic reduction of Cr(VI) using TiO₂ nanotube arrays as the photoanode and a large-area titanium mesh as the photocathode

► TNT arrays photoanode combine with Ti mesh photocathode for PEC reduction of Cr(VI). ► The complete PEC reduction of Cr(VI) to Cr(III) is achieved. ► Large-area Ti mesh photocathode is essential for the efficient reduction of Cr(VI).

**Nikesh Gupta, Henam Premananda Singh, Rakesh Kumar Sharma***Journal of Molecular Catalysis A: Chemical* 335 (2011) 248

Metal nanoparticles with high catalytic activity in degradation of methyl orange: An electron relay effect

► Metal nanoparticles (Ag, Au and Pt) of average diameter 10 nm have been synthesized via green approach. ► Degradation of methyl orange (MO) in presence of strong reducing agent such as NaBH₄ is extremely slow. ► Synthesized nanoparticles were used as a catalyst for the degradation of MO in presence of NaBH₄ and their rate constant (k) is compared. ► Rate of degradation of MO follows the order: $k_{\text{Ag nanoparticles}} \gg k_{\text{Au nanoparticles}} > k_{\text{Pt nanoparticles}} \gg k_{\text{uncatalyzed reaction}}$

**Mehdi Sheykhan, Leila Ma'mani, Ali Ebrahimi, Akbar Heydari***Journal of Molecular Catalysis A: Chemical* 335 (2011) 253

Sulfamic acid heterogenized on hydroxyapatite-encapsulated γ -Fe₂O₃ nanoparticles as a magnetic green interphase catalyst

► Magnetically recoverable catalyst leading to enhancement product purity. ► Capable biocompatible and green catalyst. ► Mild, cost-effective and applicable heterogeneous catalyst. ► Economically and environmentally benign procedure. ► Enhancement simplicity by magnetic recovery.

